

# THE AERONAUTICAL JOURNAL

Covering all aspects of Aerospace

Volume 113 Number 1141

March 2009





# THE AERONAUTICAL JOURNAL

Editor-in-chief: Prof Peter Bearman

## Associate Editors

Chairman: Prof Mike Graham

**Dr Holger Babinsky**  
Cambridge University

**Dr Trevor Birch**  
Dstl

**Professor Rene de Borst**  
Eindhoven University of Technology

**Wg Cdr Mike Bratby**  
RAeS Air Power Group

**Professor Richard Brown**  
Glasgow University

**Dr Jon Carrotte**  
Loughborough University

**Dr Graham Coleman**  
Ex-Dstl

**Professor Jonathan Cooper**  
University of Liverpool

**Mr Anthony Cross**  
BAE Systems Warton

**Professor Richard Crowther**  
Rutherford Appleton Lab

**Professor Glyn Davies**  
Imperial College, London

**Dr Olivier Dessens**  
Cambridge University

**Professor Dimitris Drikakis**  
Cranfield University

**Mr Chris Fielding**  
BAE Systems, Warton

**Professor John Fielding**  
Cranfield University

**Professor Nabil Gindy**  
University of Nottingham

**Professor Victor Giurgutiu**  
University of South Carolina

**Professor Ismet Gursul**  
University of Bath

**Professor Keith Hayward**  
RAeS Head of Research

**Professor Michael J de C Henshaw**  
Loughborough University

**Professor Richard Hillier**  
Imperial College, London

**Professor Howard Hodson**  
University of Cambridge

**Mr Julian Lea-Jones**  
Systems Consultant

**Professor Ken Morgan**  
University of Wales, Swansea

**Dr Ravi Nayak**  
National Aerospace Laboratories, India

**Professor Gareth Padfield**  
University of Liverpool

**Dr Shahrokh Shahpar**  
Rolls-Royce

**Professor Constantinos Soutis**  
University of Sheffield

**Professor John Stollery**  
Cranfield University

**Professor Anthony Waas**  
University of Michigan

### Aims and scope

The aims and scope of *The Aeronautical Journal* are intended to reflect the objectives of the Royal Aeronautical Society as expressed in its Charter of Incorporation. Briefly, these are to encourage and foster the advancement of all aspects of aeronautical and space science. Thus the topics of *The Aeronautical Journal* include most of those covered by the various Specialist Groups of the Society, which include:

Aircraft design, aerodynamics, air law, air power, air transport, air navigation, airworthiness and maintenance, aviation medicine, avionics and systems, environmental issues, flight operations, flight simulation, fluid dynamics, fluid mechanics, general aviation, guided flight, human factors, human powered flight, light aviation, management studies, propulsion, rotorcraft, safety, space, structures and materials, structural mechanics, systems and test procedures and UAVs.

Papers are therefore solicited on all aspects of research, design and development, construction and operation of aircraft and space vehicles. Papers are also welcomed which review, comprehensively, the results of recent research developments in any of the above topics.

We recognise the inhibiting pressures of time and confidentiality and acknowledge that many of the design testing, manufacturing and operational problems that industry has to solve contain important information for the whole aerospace community. *The Aeronautical Journal* provides a platform for refereeing and presenting your work to an international audience.

Papers will be considered for publication in *The Aeronautical Journal* if they meet the terms and conditions listed in The Instructions for authors. If these are not met, the Editor reserves the right to withdraw the paper without redress, which may be at any time up to publication.

Papers should be sent to: Prof Peter Bearman, Royal Aeronautical Society, No. 4 Hamilton Place, London W1J 7BQ, United Kingdom.

### Subscriptions

#### Non-members

Annual subscription (12 issues) £390, Single copies, including back issues £36; *Non-member subscription orders are available from*; Royal Aeronautical Society, Publications Subscriptions Department, Dovetail Services Ltd, 800 Guilla Avenue, Kent Science Park, Sittingbourne, Kent ME9 8GU, UK.

Tel: +44 (0)844 848 8426, Fax: +44 (0)844 856 0650, email: ras@servicehelpline.co.uk

#### RAeS members

Annual subscription (12 issues) £65, Single copies, including back issues £6; *member subscription orders are available from*; Membership Department, Royal Aeronautical Society, No. 4 Hamilton Place, London W1J 7BQ, UK. Tel: +44 (0)20 7670 4300, Fax: +44 (0)20 7670 4309, email: membership@aerosociety.com

#### RAeS Conference Proceedings

Details, price and availability of Royal Aeronautical Society Conference Proceedings can be obtained from; RAeS Conference and Events Department, No. 4 Hamilton Place, London W1J 7BQ, UK. Tel: +44 (0)20 7670 4300, email: conference@aerosociety.com or via [www.aerosociety.com/proceedings](http://www.aerosociety.com/proceedings)

**All papers are available to view free of charge for subscribers and to purchase by others at: [www.aerosociety.com](http://www.aerosociety.com)**





# CONTENTS

Volume 113 Number 1141

Reproduction of any of the papers published in this journal is not permitted without the written consent of the Editor.

**Editor-in-Chief**

Professor P W Bearman FREng, FCGI, FRAeS

**Managing Editor**

C S C Male BSc(Eng) MRAeS

**Production Editor**

W J Davis BA ARAeS

**Publications Officer**

A L Hallam BA ARAeS

**Production**

W I I Read MA(Econ)  
T C Robinson BA

**Book Review Editor**

B L Riddle BLib

**Publisher**

Royal Aeronautical Society (RAeS)  
No.4 Hamilton Place  
London W1J 7BQ, UK  
Tel: +44 (0)20 7670 4300  
Fax: +44 (0)20 7670 4359  
e-mail: publications@aerosociety.com  
raes@aerosociety.com

<http://www.aerosociety.com>

The Royal Aeronautical Society  
is a registered charity: No 313708

**RAeS Chief Executive**

K D R Mans BA FRAeS

The content does not necessarily express the opinion of the Council of the Royal Aeronautical Society.

**Advertisement Sales**

David Lancaster, Group Sales Manager  
Ten Alps Publishing  
9 Savoy Street  
London WC2E 7HR, UK  
Tel: +44 (0)20 7878 2316  
Fax: +44 (0)20 7379 7118/7155  
email: david.lancaster@tenalpspublishing.com

**Printer**

Manor Creative Limited  
7 and 8 Edison Road  
Eastbourne  
East Sussex  
BN23 6PT  
United Kingdom  
ISSN: 0001-9240

Published monthly



**Mixed Sources**  
Product group from well-managed  
forests and other controlled sources  
[www.fsc.org](http://www.fsc.org) Cert no. TF-COC-002794  
© 1996 Forest Stewardship Council

**D.I.A. Poll**

The optimum aeroplane and beyond

151

**S.K. Krishnababu, H.P. Hodson, W.N. Dawes,  
P.J. Newton and G.D. Lock**

Numerical and experimental investigation of tip leakage flow and heat transfer using idealised rotor-tip models at transonic conditions

165

**K. Ghorbanian, M.R. Soltani, M.D. Manshadi and M. Mirzaei**

Control of separation in the concave portion of contraction to improve the flow quality

177

**S. De Jesus-Mota, M. Nadeau Beaulieu and R.M. Botez**

Identification of a MIMO state space model of an F/A-18 aircraft using a subspace method

183

**Y. Cao, Z. Wu, Q. Song and J. Sheridan**

Numerical simulation of fluid-structure interaction in the opening process of conical parachute

191

**Book Reviews**

202

Front cover: Shown is a concept future airliner as imagined by the RAeS and realised by graphic design studio, Kaktus Digital ([www.kaktusdigital.com](http://www.kaktusdigital.com)).

[Reprinted from THE AERONAUTICAL JOURNAL OF THE ROYAL AERONAUTICAL SOCIETY, MARCH 2009]

# Numerical simulation of fluid-structure interaction in the opening process of conical parachute

**Y. Cao, Z. Wu and Q. Song**

**yihuacs@yahoo.com.cn**

Institute of Aircraft Design

Beijing University of Aeronautics and Astronautics

Beijing, China

**J. Sheridan**

Department of Mechanical and Aerospace Engineering,

Faculty of Engineering, Monash University

Victoria, Australia



# Numerical simulation of fluid-structure interaction in the opening process of conical parachute

Y. Cao, Z. Wu and Q. Song

yihuacs@yahoo.com.cn

Institute of Aircraft Design

Beijing University of Aeronautics and Astronautics

Beijing, China

J. Sheridan

Department of Mechanical and Aerospace Engineering,

Faculty of Engineering, Monash University

Victoria, Australia

## ABSTRACT

According to multi-node model, the dynamics equations of conical parachute system for simulating shape deformation process of the flexible canopy in the opening process were established. With the combination of dynamics equations code and computational fluid dynamics (CFD) software, the fluid-structure interaction investigation of the conical parachute was carried out. Also the change of parachute shape and flow field, inflation time, the rate of descent, the distance of descent, and other relevant data were achieved. This paper has focused on analysing vortex structure of the flow field in the opening process of conical parachute, and laid the foundation for studying mechanics mechanism of flow field variation of conical parachute in future.

## NOMENCLATURE

$a_{sy}$	vertical acceleration value of entire parachute system
$a_x(i)$	acceleration values of node $i$ in $X$ direction
$a_y(i)$	acceleration values of node $i$ in $Y$ direction
$D$	inflation force
$dp$	pressure difference between inner and outer canopy surface
$E_b$	elastic modulus of canopy weave
$FL$	elastic force along longitude
$FL(i)$	elastic force along longitude between node $i$ and node $i-1$
$Fp$	air pressure
$Fu$	elastic force along latitude

$Fu(i)$	elastic force of node $i$ along latitude
$g$	acceleration of gravity
$K$	shrink factor of canopy material
$L$	distance between two neighboring nodes
$M$	mass of recovery payload
$m(i)$	mass of node $i$
$S$	area of cirque when inflated
$T$	force on suspension line
$V_0$	initial velocity
$\alpha(k)$	angle between $X$ axis and normal direction of line $k$
$\epsilon_m$	strain in longitudinal direction
$\epsilon_u$	strain in latitudinal direction
$\sigma_m$	stress in longitudinal direction
$\sigma_u$	stress in latitudinal direction
$\theta$	angle between suspension line and $Y$ axis

## 1.0 INTRODUCTION

As an effective deceleration appliance, parachute is widely used in aeronautics, astronautics, sports and other fields. The security of aviation can be effectively improved by enhancing the capabilities of parachutes. In the last decades, fluid-structure interaction problem of parachute has been studied widely to meet both the public need for airliner security and military aviation. Along with the progress of computational technology and computer engineering, many models



have been developed recently to solve the dynamics problem of parachute systems. A computational method based on the parallel finite element algorithm was proposed by Stein *et al* (1997)<sup>(1)</sup>. They simulated a three-dimensional (3D) model for the flat circle parachute under the assumptions that the canopy of parachute is fully inflated as a hemisphere with a vent on the top. They have achieved a feasible computational solution of parachute problems. Most recently, they revised their model (2000)<sup>(2)</sup>, and obtained some important parameters of flow field including pressure and velocity. Following the same principles and similar numerical method, Kalro and Tezduyar set up a parafoil model (2000).

The whole process of parachute dropping is divided into three phases: deployment, inflation and terminal descent. And the inflation phase is most complicated. It is because parachute canopy in the inflation, which is flexible fabric, undergoes a prominent structure deformation in a short period of time. At the same time, the flow field inside and outside canopy has complicated changes. And the coupling of the both fluid and structure makes the inflation phase more intricate. In a word, the parachute inflation is a fluid-structure interaction problem which relates to structure deformation and flow field change, as well as the interactive effects of the both. Earlier fundamental work was done in 1942 by Pflanz<sup>(3)</sup>. He integrated the non-linear differential equation of motion and calculated the inflation force for the simplified case. Following this, O'Hara noted the opening behaviour and the opening forces of parachute inflation<sup>(4)</sup> in 1949, which are recently focused on by the last researchers. Thereafter a lot of engineering algorithms, numerical algorithms and experiments were used on the parachute inflation. And Ludtke's work is worth notice. In 1973 he applied Pflanz's solution for the opening force factor to analysis of circular flat canopies<sup>(5)</sup>. The more general case and the effect of over-inflation were treated by Ludtke in 1986<sup>(6)</sup>. Recently the researchers focus on the fluid-structure interaction of the parachute inflation. Norio and Kensaku tried to catch numerically the flow structure around the flexible body, which could be deformed by the textile tension<sup>(7)</sup>.

So far, most of the research works have been generally focused on the simulation and analyses of flat circle parachutes using the parallel finite element algorithm<sup>(8)</sup>. However, few works have been done to simulate more complicated parachute models<sup>(9-10)</sup>, such as the conical parachute, a typical parachute widely used in aviation utilization, especially for the inflation phase of conical parachute.

Based on the above cases, a try is made in this paper. One real conical parachute system is first simplified. Then the multi-nodes model of parachute system and computational fluid dynamics (CFD) software are established for numerically simulating the opening process of the conical parachute. The flow field changes, the canopy shape and other relevant data in inflation phase are obtained. Finally, the development process of vortex structure in the opening process of the parachute are focused on and analysed.

## 2.0 SIMPLIFICATION OF THE MODEL OF CONICAL PARACHUTE SYSTEM

The flow field of parachute is complicated and unsteady. The interface of fluid and solid for parachute is dynamic, and the canopy is permeable. All above factors increase the difficulty of numerical simulation. As for the establishment of conical parachute model, the assumptions to appropriately simplify conical parachute system are set as follows:

### 2.1 Quasi-steady assumption

It is well known that apex vent (i.e. upper hole) with suitable size on hollow hemisphere could greatly weaken the unsteadiness of its flow field<sup>(11)</sup>, or even eliminate the unsteadiness caused by vortex at all. In this study, a parachute model with apex vent whose diameter

accounts for 5% of the canopy diameter is chosen, so the unsteadiness is not quite influential<sup>(12)</sup>.

CFD method was applied to calculate the flow field characteristics. Quasi-steady assumption is adopted here. It is meant that with focus on the simulation of fluid-structure interaction, whole unsteady process in opening process is divided into  $n$  time ( $t_1 \dots t_j \dots t_n$ ) states. As for  $t_j$  state, all physical variables in CFD equations are first solved with a steady treatment and taken as the values of time  $t_j$  and then FSI calculation is accomplished. Because using the tiny time step, the flow is assumed to be steady during each state. On the entire FSI process, the flow and structure are changing over time.

### 2.2 The simplified flow field assumption

The decline rate of parachute is generally less than  $50\text{ms}^{-1}$  in the inflation process. Therefore the parachute flow is typical incompressible flow. Parachute system is a self-balance system in the actual course of decline, and it is in a state of slow swing within the extent of small angles-of-attack. This paper assumes that the angle-of-attack is kept same.

### 2.3 The simplified conical parachute structure assumption

The porosity of canopy is not considered in the calculation of parachute flow field. The parachute canopy is simplified to be a symmetry body of rotation (see Fig. 1 through Fig. 3). The structure deformation and flow field were calculated and discussed in two-dimensional symmetrical case. Canopy and rope produce no force when bended, the mass and strain of rope are ignored. The pressures only change along longitudinal line, but keep same along latitudinal line.

The size of the simplified conical parachute model, the physical layout of no-inflatable model, and the side elevation of inflatable model are shown in Fig. 1 through Fig. 4.

The parameters of the system are as follows:

Radius of canopy:	3.4m
Radius of apex hole:	0.175m
Length of rope:	6.4m
Mass of canopy:	10kg
Mass of payload:	90kg
Temperature:	300K
Air density:	1.225
$E_b$ :	29,169N/m
$K$ :	0.47
Initial velocity:	$50\text{ms}^{-1}$
$g$ :	$9.8\text{ms}^{-2}$
Angle-of-attack:	$0^\circ$

## 3.0 MULTI-NODE MODEL

In this paper canopy structure model is used to solve stress and displacement of the canopy, and to get the canopy shape in a moment of the inflation process. For any moment of the parachute inflation process virtual inertial force is applied on the canopy according to D'Alembert's principle, so that the dynamics problem is transformed to the static equilibrium one. Therefore, if a structure model, which is easy to calculate and maintain the mechanical properties of parachute, was established, the fluid-structure interaction process, which is referred to Section 4, is iterated to get the flow field of the inflation process at this moment.

### 3.1 Establishment of the multi-node model

As the structure of simplified conical parachute is an axial symmetry one, and the inflation is symmetric, then the structure deformation



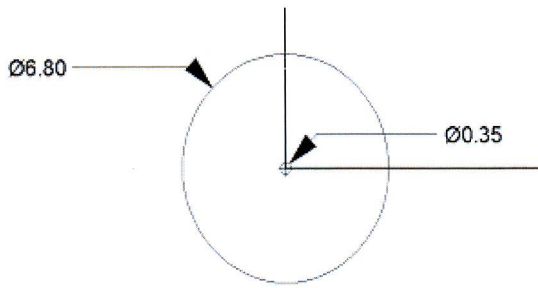


Figure 1. The size of the simplified conical parachute model (unit: m) top view.

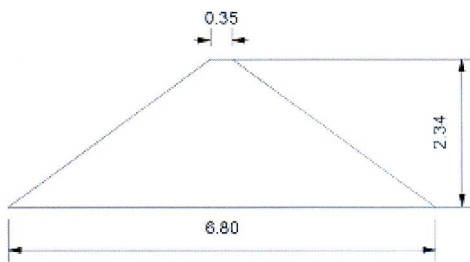


Figure 2. The size of the simplified conical parachute model (unit: m) front view (below).

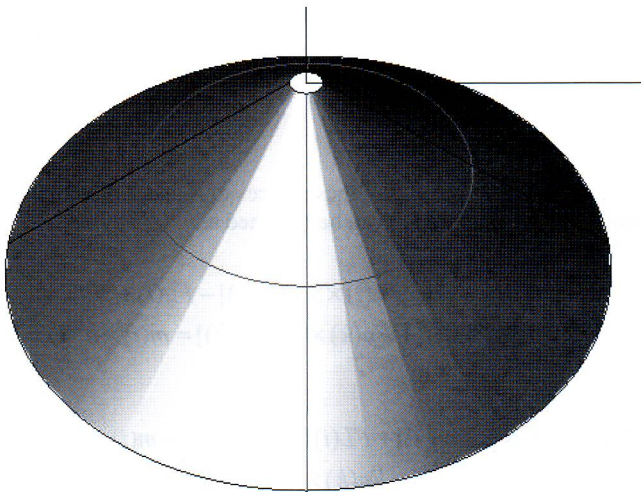


Figure 3. The physical layout of no-inflatable model.

and corresponding flow field of the model is also axial symmetrical. Therefore the shape of an arbitrary longitudinal line on the canopy would represent the shape of parachute. In the structure model, the canopy laid flatwise is divided into  $N$  cirques along radial direction, and mass of every cirque is concentrated to the point where 0 degree longitudinal line crosses with the middle circle of this cirque, so we get  $N$  mass nodes along 0 degree longitude, as shown in Fig. 5. When inflated, the forces caused by air pressure and strain are also concentrated to these mass nodes, and they should be projected to  $X$  and  $Y$  directions. In doing so, the two-dimensional symmetrical multi-node structure model of canopy is constructed.

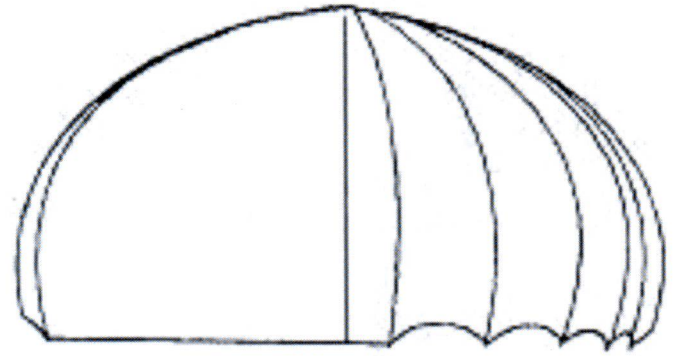
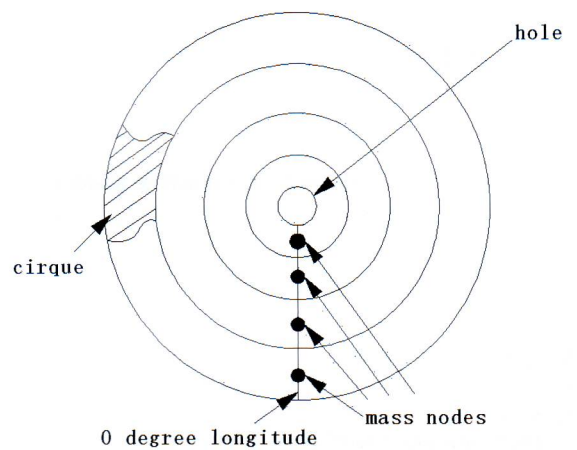
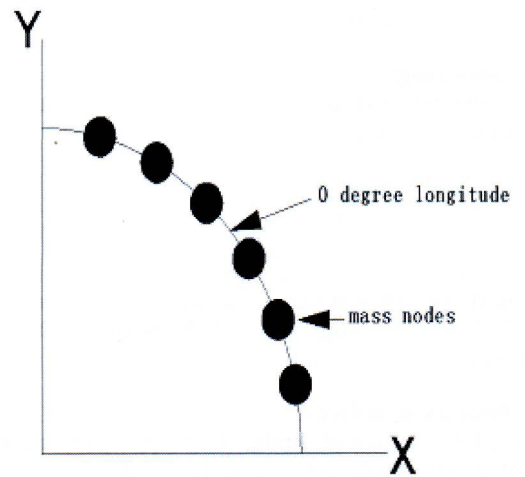


Figure 4. The side elevation of inflatable mode <sup>(13)</sup>.



(a) Top view when laid flatwise.



(b) Side view when inflated.

Figure 5. Multi-node model of canopy.



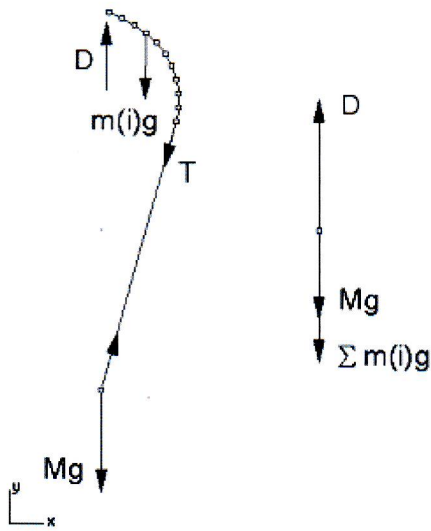


Figure 6. Multi-node model of parachute system.

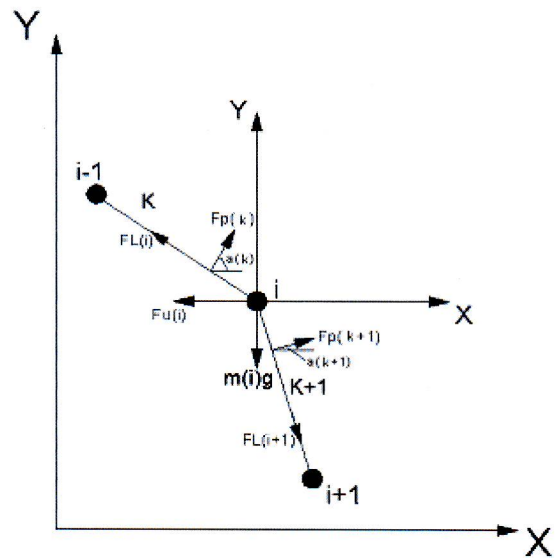


Figure 7. Forces on node *i*.

A mass point could be used to represent the payload whose mass is *M*, and it is connected with the multi-node model of canopy by weightless and inextensible rope, as shown in Fig. 6. These modules construct the multi-node model of parachute system.

**3.2 Establishment of the dynamic equations of the multi-node model**

**3.2.1 Force of parachute system**

**Gravity force:**

*G*, caused by gravity, equals  $m \times g$ .

**Elastic force along longitude:**

*FL*, caused by longitudinal strain of canopy<sup>(14)</sup>, represented by the change of distance between two neighbouring nodes,

$$FL = 2\pi\sigma_m X = \frac{E_b[\epsilon_m + K\epsilon_u]}{1 - K^2} 2\pi X \quad \dots (1)$$

where  $\sigma_m$ ,  $\epsilon_m$  are respectively stress and strain in longitudinal direction;  $\sigma_u$ ,  $\epsilon_u$  represent stress and strain in latitudinal direction; *K* is shrink factor of canopy material. *E<sub>b</sub>* is the elastic modulus of canopy weave.

**Elastic force along latitude:**

*Fu*, caused by latitudinal strain of canopy<sup>(14)</sup>, represented by the change of *X* co-ordinate value of the mass node,

$$Fu = \sigma_u L = \frac{E_b(\epsilon_u + K\epsilon_m)}{1 - K^2} L \quad \dots (2)$$

*L*: distance between two neighbouring nodes.

**Pressure:**

*Fp*, caused by air pressure, equals  $dp \times S$ , *dp* is the pressure difference between inner and outer canopy surface, *S* is the area of cirque when

inflated. A group of straight lines between nodes are used to represent longitudinal curve. The pressure on a node can not be projected to the curve's normal direction because two straight lines get together here. Therefore the sum of half pressure vectors on its two neighbouring cirques is used to substitute the normal direction pressure.

**3.2.2 Equations of canopy**

According to Fig. 7, projecting these forces to *X* and *Y* directions, the dynamic equations of node *i* can be obtained as:

In *X* direction:

$$FL(i+1) \times \sin[\alpha(k+1)] - FL(i) \times \sin[\alpha(k)] - Fu(i) + Fp(k+1) \times \cos[\alpha(k+1)] + Fp(k) \times \cos[\alpha(k)] = m(i) \times a_x(i) \quad \dots (3)$$

In *Y* direction:

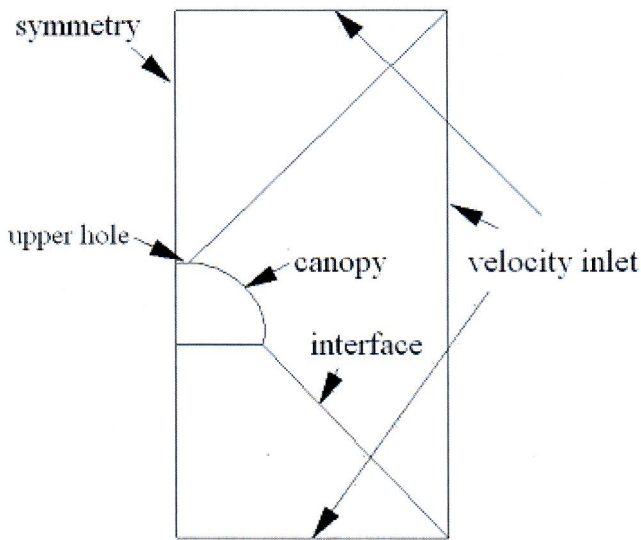
$$-FL(i+1) \times \cos[\alpha(k+1)] + FL(i) \times \cos[\alpha(k)] - m(i) \times g + Fp(k+1) \times \sin[\alpha(k+1)] + Fp(k) \times \sin[\alpha(k)] = m(i) \times a_y(i) \quad \dots (4)$$

$\alpha(k)$  is angle between *X* axis and normal direction of line *k*.  $a_x(i)$ ,  $a_y(i)$ , are acceleration values in *X* and *Y* directions.

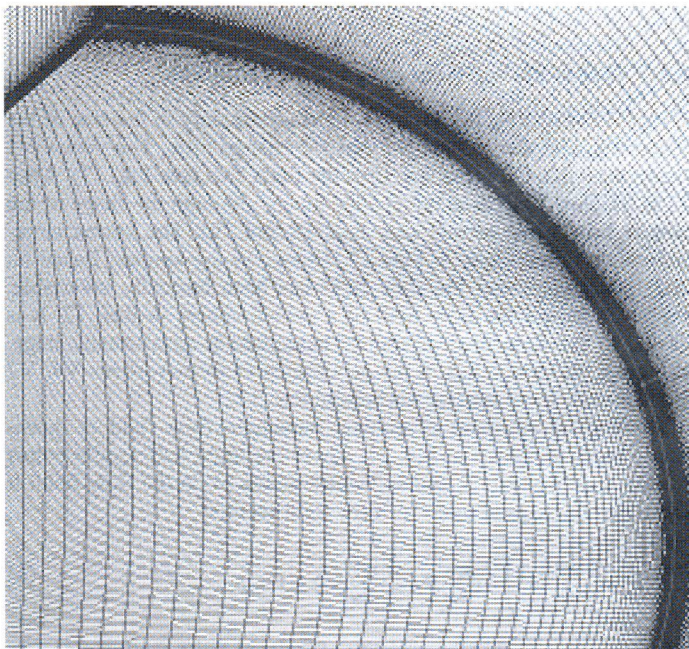
According to the known velocity of the node *i* at the initial moment, and assuming the motion of the node *i* was uniform variation motion within a period time  $\Delta t$ , the node's acceleration can be calculated from the force on the node and the above equations, and the displacement and velocity of the node after  $\Delta t$  can be obtained through the equations of uniform variation motion. Through the integration for the time increment  $\Delta t$ , the co-ordinates and velocity of the node *i* can be got. As is well known, the forces on the nodes change continuously with time. It is because the air pressure *Fp* varies with the flow field that changes with time, and the elastic forces *FL* and *Fu* vary with the location of the nodes.

Nodes correlate with each other by elastic forces. After getting such equations on each node and assembling them all together, the dynamic equations of the canopy model were established.





(a) Computational area



(b) Body fitted grid of canopy

Figure 8. Computational grid at 0.5s.

### 3.2.3 Equations of entire system

Because the rope is inextensible, the entire system could be supposed to descend with the same acceleration, and therefore an equation for the parachute system in the vertical direction ( $Y$ ) can be constructed as:

$$D - M \times g - \sum [m(i) \times g] = [M + \sum m(i)] \times a_{sY} \quad \dots (5)$$

$a_{sY}$  is vertical acceleration values of entire parachute system.

According to the method mentioned in 3.2.2 Equations of canopy, the co-ordinates and velocity of the entire system can be got at any moment.

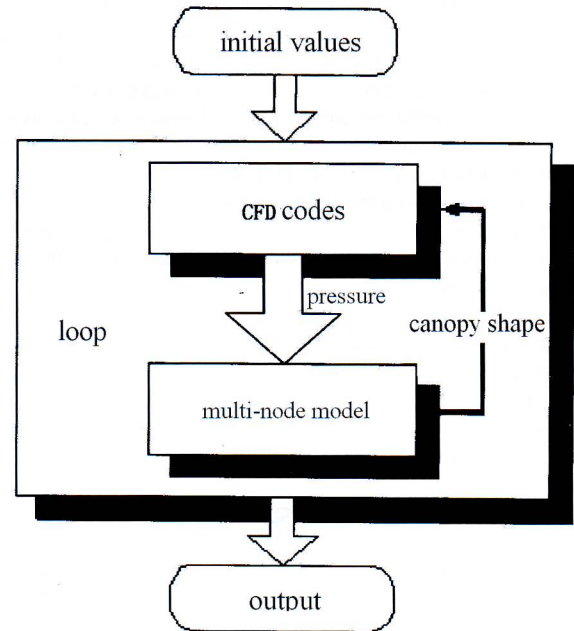


Figure 9. Procedure of fluid-structure interaction.

The equations of parachute system consist of the equations of canopy and equation of the entire system. The simulation of the structure distortion in the parachute inflation is transformed into solving the above equations, and the position, velocity, acceleration, and other relative data of each node and the parachute system can be obtained at any moment.

## 4.0 FLOW FIELD CALCULATIONS AND FLUID-STRUCTURE INTERACTION

This paper uses the independent code to solve the equations of parachute system multi-node model, and the CFD codes to calculate the flow field of the parachute at every step. According to the possible circulating flow, this paper chooses the RNG  $k - \epsilon$  turbulent model.

Computational grid at 0.5s is shown in Fig. 8.

The fluid-structure interaction procedure of parachute at any time in the inflation process is shown in Fig. 9.

The input parameters of FSI are as follows:

- Velocity of parachute system : change with the steps of FSI;
- Angle between suspension line and  $Y$  axis ( $\theta$ ): change with the steps of FSI;
- Mass of every node: constant;
- Distance between adjacent nodes without deformation: constant;
- Abscissa of every node without deformation: constant;
- Velocity of every node at the end of last step: change with the steps of FSI;
- Elastic force along longitude of adjacent nodes at the end of last step: change with the steps of FSI;
- Elastic force along latitude of adjacent nodes at the end of last step: change with the steps of FSI;
- Pressure of every node from CFD calculation at this step: change with the steps of FSI.



With structure model and descent velocity given at initial moment, the air pressure could be calculated using CFD codes. Then, by solving dynamic equations of parachute system multi-node model with the calculated air pressure values, the shape of parachute and descent velocity could be calculated and renewed. Following this step, the new shape and descent velocity would then be sent to CFD codes for the new calculation of air pressure values again.

Repeating this procedure with a time increment of 0.01s (when severe change happens) or 0.02s (when slight change happens), the changes of canopy shape and descent characteristics in the inflation process could be obtained.

At initial moment, the parachute has been straightened by guidance surface parachute. Unlike the usually adopted arc-line model, a single line with anti-clockwise 3 degree angle against negative  $Y$  direction is used as the initial model of canopy. In fact, this model is more like the canopy outline when inflation begins.

## 5.0 RESULTS ANALYSES

The simulation starts at 0s. At 1.25s, the descent velocity of parachute system is  $11.504278\text{ms}^{-1}$ , with acceleration of  $-0.645427\text{ms}^{-2}$ . Because the change of velocity and canopy shape is very slight during a long period after 1.25s, the state at 1.25s is considered as the beginning of steady descent states. In this way the simulation of inflation process ends.

### 5.1 Canopy deformation

Canopy deformation from 0s to 0.59s is shown in Fig. 10, and shape change is very slight after 0.59s.

As can be seen in the graphs, the deformation is not simply expansive; a course of expansion-shrink-expansion exists, which is especially obvious when comparing shapes at 0.14 and 0.15s. The upper part of canopy at 0.15s shrinks inside relative to the outline at 0.14s. This phenomenon looks like a breath process of canopy, so it was called canopy breathing<sup>(15)</sup>. And it also happens at 0.31s, 0.33s and 0.35s.

As for analysing change of stress values when canopy breathing happens, the reason why such phenomenon exists can be concluded. At first, inflation force rises rapidly; shape of canopy also changes greatly, and results in severe stress; then, the inflation force declines steeply to a value which is unable to retain the outline against stress, so the canopy would shrink because of stress.

The shape of canopy changes greatly from 0.0s to 0.35s, especially from 0.0s to 0.07s. When to 0.35s, the shape changes little, and the variation rate of the parachute system reduces significantly. After the inflation, the stable shape of canopy (Fig. 10(f)) is similar to the side elevation of inflatable model (Fig. 4) in Ref. 13. It proves that the multi-node model is correct in the simulation of the conical parachute inflation.

### 5.2 Flow field change

In the parachute inflation, the characteristics of the flow field changes very quickly. In 1.25s, the velocity of the conical parachute reduces from  $50\text{ms}^{-1}$  to about  $11\text{ms}^{-1}$ ; the canopy has also experienced a great deformation. The in-depth study of this process requires a large amount of calculation and a long period of data collection. After analysing the streamline pattern at different times, we can divide the flow process into three stages: the preliminary formation stage, the full development stage and the quasi-steady flow stage.

#### 5.2.1 Preliminary formation stage (0s to 0.05s)

From 0s to 0.02s the flow pattern is almost flat with anti-clockwise 3 degree angle against the flow. A vortex, named V1 in Fig. 11, grows at the end of canopy, and produces pressure difference which

promotes canopy to expand outside. It should be noted that there is not any vortex in the pane of Fig. 11. It is just a reattachment zone. But with the passage of time, the edge of upper hole is inflated more greatly, and a new vortex, named V2 in Fig. 12, grows in the reattachment zone at 0.03s. At 0.04s the vortex V1 is divided into two vortices, and another new vortex, named V3 in Fig. 13, separates from the vortex V1. The different grade inflation brings a corner on the canopy, and the corner is the main reason of the separation of the vortex V1 which firmly attaches to the canopy. At the same time the vortex V2 grows bigger. All above are showed distinctly in Fig. 13. When it comes to 0.05s, the vortex V3 has grown as big as the vortex V1, and the structure of the three vortices has already been formed in the flow field of conical parachute.

#### 5.2.2 Full development stage (0.06s to 0.12s)

From 0.06s to 0.11s, the flow field changes mainly in the location and size of the three vortices. Contrasting between the flow field at 0.05s and 0.11s, we could find that the vortices V2 and V3 keeps growing, and are bigger than the vortex V1 which attaches to the canopy part without inflating (see Fig. 16). As the canopy keeps inflating, the uninflated part and the vortex V1 is decreasing. Until it comes to 0.12s, the vortex V1 is absorbed by the vortex V3 and disappears (see Fig. 17). At the same time, the top jet passing the vortex V2 joints into the outflow and rolls up a new vortex V4 in the downstream. A new structure of the three vortices has already been formed in the flow field of conical parachute.

#### 5.2.3 Quasi-steady flow stage (0.13s to 1.25s)

From 0.12s to 0.15s, the fluid field changes mainly in the size of the vortex V4, and the vortices V2 and V3 change little. The vortex V4 grows very fast to bigger size than the other two (see Fig. 17). After 0.15s the flow field does not change much, although the shape of the canopy transforms greatly (see Figs 18 and 19). The vortex structures of the flow fields in Figs 17, 18 and 19 are similar. Based on this, it is judged that the flow field has been basically invariable. Figure 20 shows the flow field of a vented sphere in Ref. 12. It is similar to the flow field of conical parachute at quasi-steady stage. The great difference lies in the occurrence of three vortices V4, V2 and V3 while there are two vortices in Ref. 12.

Topological structure of conical parachute flow field at quasi-steady stage is shown in Fig. 21. There are eight half saddle points  $S'$ , four saddle points  $S$ , and six centre points  $Nc$  in the flow field. It obeys the topological rule<sup>(16)</sup> of flow field section:

$$\left( \sum N + \frac{1}{2} \sum N' \right) - \left( \sum S + \frac{1}{2} \sum S' \right) = 1 - n \quad \dots (6)$$

Where  $n = -m + 1$ .  $m$  is the quantity of isolated finite section plane. In this situation,  $m = 2$ ,  $n = 3$ . Moreover, along the symmetry axis there are two saddle points  $S$  for the conical parachute flow field, which is same as that in the flow field of vented sphere in Fig. 20.

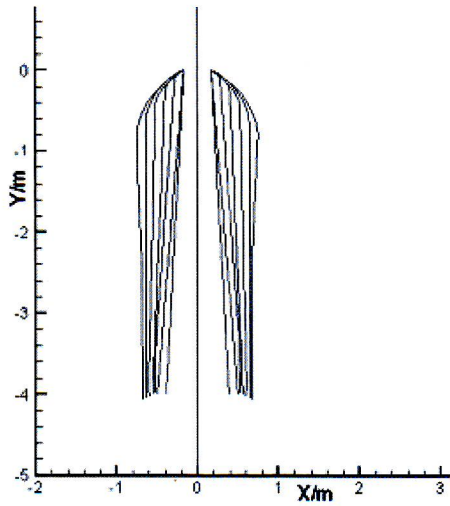
### 5.3 Characteristics change

The simulation starts at 0s. At 1.25s, the descent velocity of parachute system is  $11.504278\text{ms}^{-1}$ , with acceleration of  $-0.645427\text{ms}^{-2}$ . Because the change of velocity and canopy shape is very slight during a long period after 1.25s, the state at 1.25s is considered as the beginning of steady descent states. In this way, the simulation of inflation process ends.

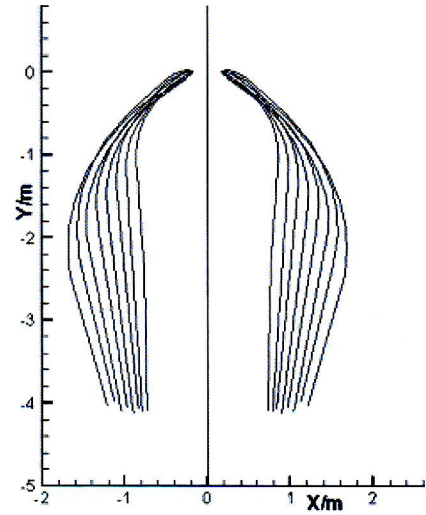
The change of inflation force is shown in Fig. 22.

The inflation force result gained through multi-node model is similar to the typical curve in Fig. 23 of Watkins's report<sup>(17)</sup>. The value rise sharply at the beginning, reach first apex (15,064.07N) called snatch force at 0.16s, then suddenly decline, but it rise rapidly

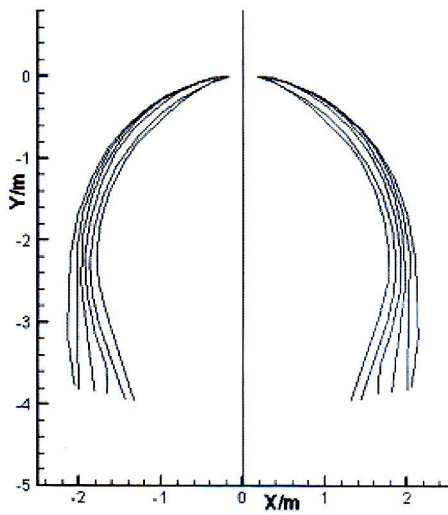




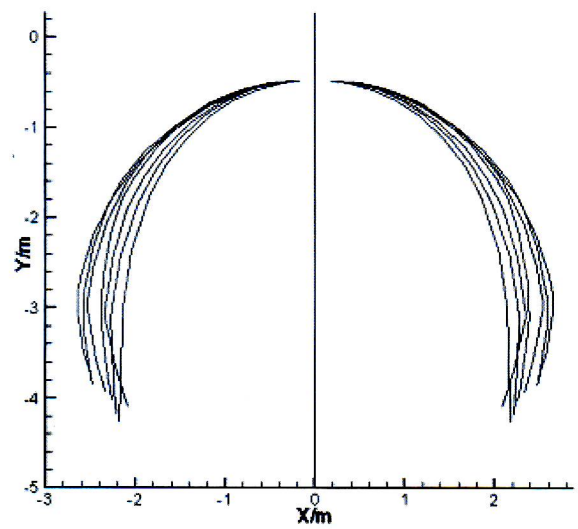
(a) 0s to 0.07s (interval = 0.01s, without 0.01s).



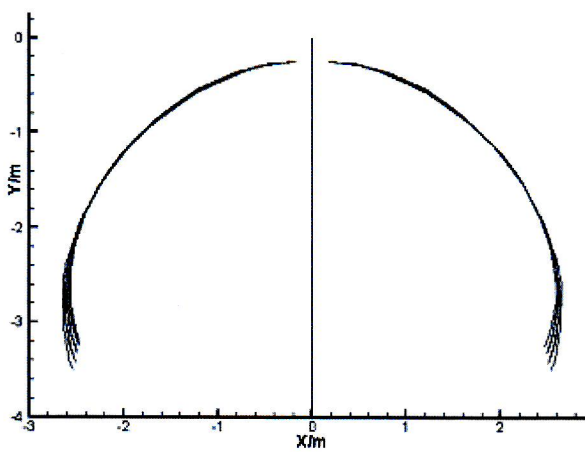
(b) 0.08s to 0.15s (interval = 0.01s).



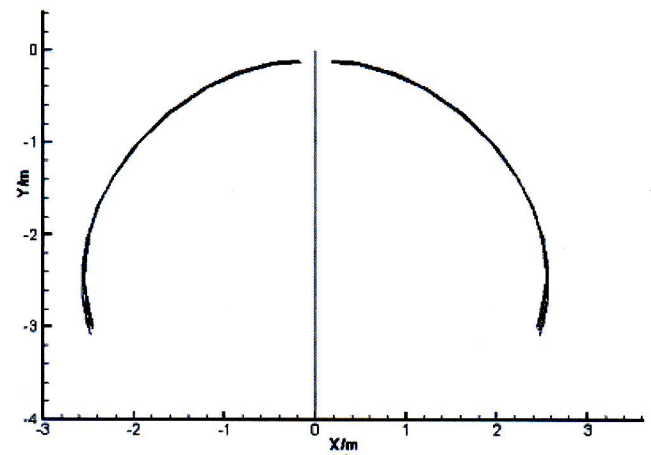
(c) 0.16s to 0.21s (interval = 0.01s).



(d) 0.23s to 0.35s (interval = 0.02s).



(e) 0.37s to 0.47s (interval = 0.02s).



(f) 0.49s to 0.59s (interval = 0.02s).

Figure 10. Change of canopy shape (portion).



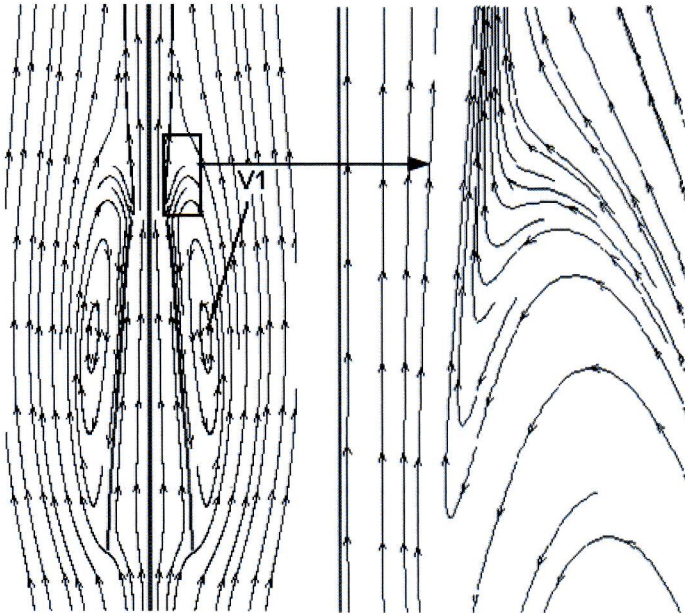


Figure 11. Streamlines near canopy at 0.02s, preliminary formation stage (the right picture is the enlargement of the pane in left picture).

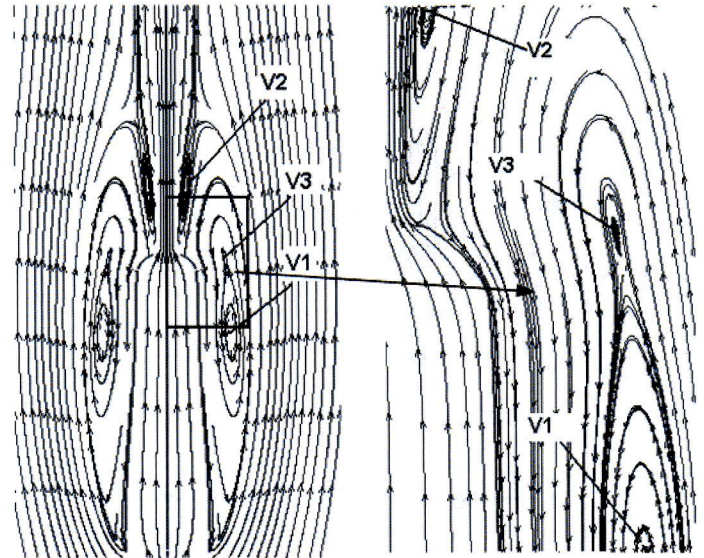


Figure 13. Streamlines near canopy at 0.04s, preliminary formation stage (the right picture is the enlargement of the pane in left picture).

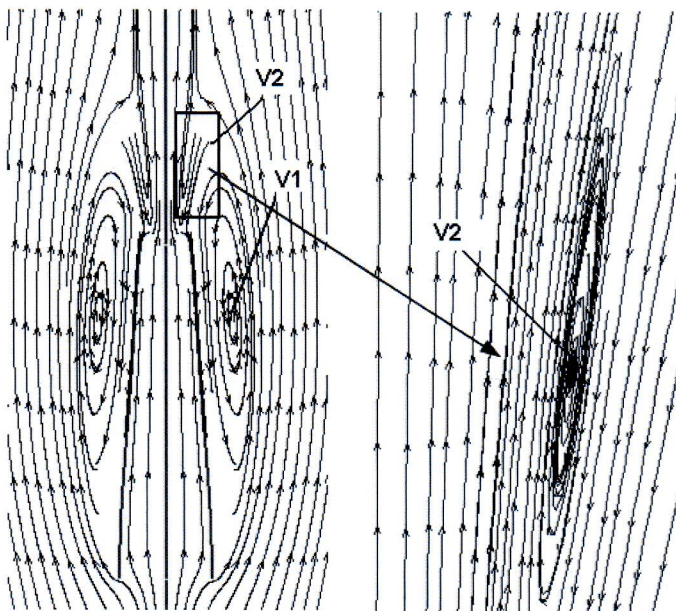


Figure 12. Streamlines near canopy at 0.03s, preliminary formation stage (the right picture is the enlargement of the pane in left picture).

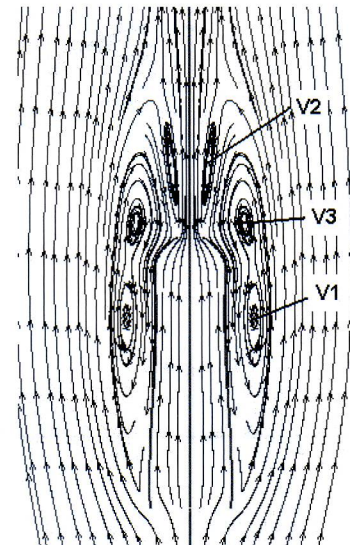


Figure 14. Streamlines near canopy at 0.05s, preliminary formation stage.

again to the second apex named peak inflation force at 0.21s, with a bigger value (17669.85N). After 0.21s, inflation force falls fast, then, after about 0.8s, its value reaches a relatively steady count (1,832.45N).

Change of descent velocity is shown in Fig. 24. The velocity is  $50\text{ms}^{-1}$  at 0s (i.e. the beginning of inflation process), falling to  $11.504278\text{ms}^{-1}$  at 1.25s when inflation process is relatively steady (i.e. simulation for inflation process ends).

In order to evaluate the results, the work of Garrard has been selected<sup>(18)</sup>. He reported on a 10.5m diameter conical parachute used to recover 162.5kg mass from a velocity of  $55.5\text{ms}^{-1}$  to  $8\text{ms}^{-1}$  (approximate). His inflation lasted 1.3s, and the maximum force is 10,411.123N. The above computed result shows a good agreement between the present work and the work of Garrard.

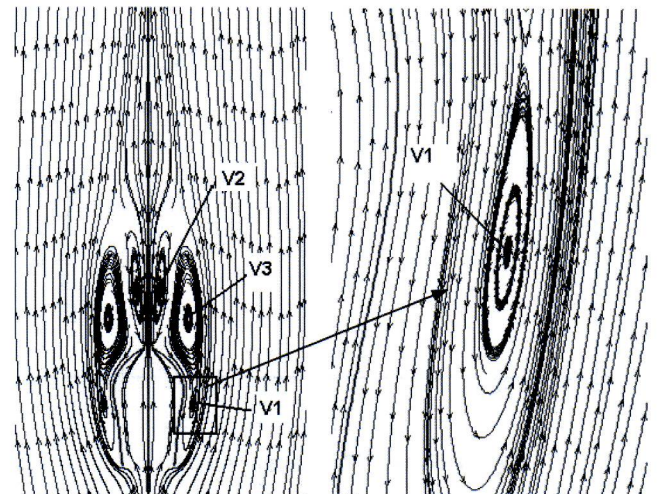


Figure 15. Streamlines near canopy at 0.11s, full development stage (the right picture is the enlargement of the pane in left picture).



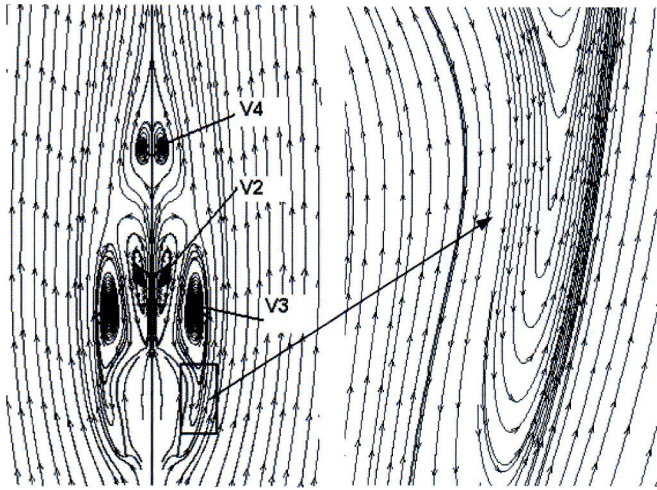


Figure 16. Streamlines near canopy at 0.12s, full development stage (the right picture is the enlargement of the pane in left picture).

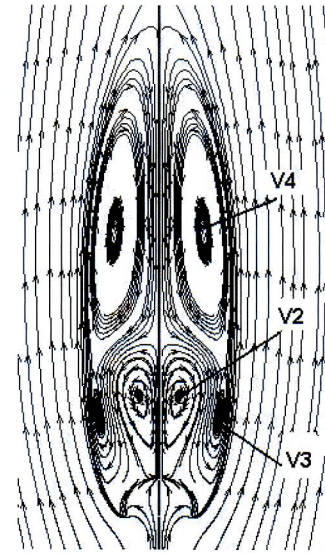


Figure 19. Streamlines near canopy at 0.59s, quasi-steady stage.

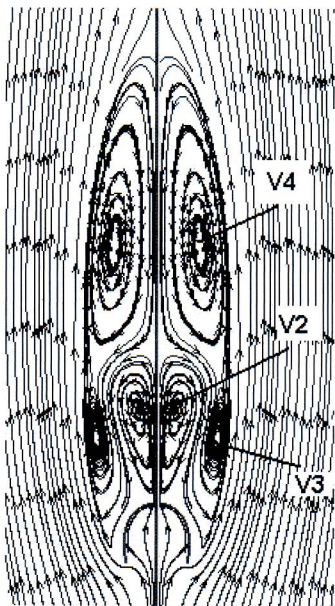


Figure 17. Streamlines near canopy at 0.15s, quasi-steady stage.

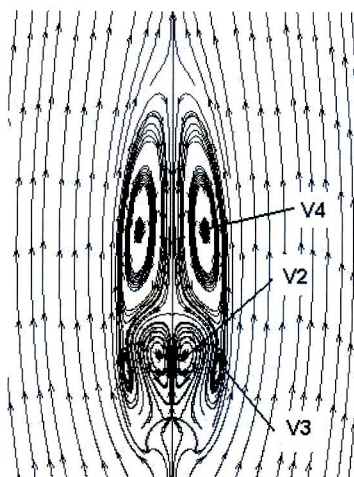


Figure 18. Streamlines near canopy at 0.35s, quasi-steady stage.

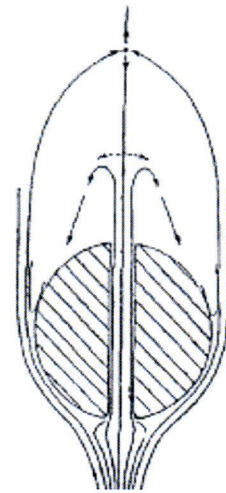


Figure 20. The flow field of vented sphere<sup>(12)</sup>.

However, as some initial parameters, such as the radius of canopy, mass of payload and initial velocity, are different, some results in the present work do not agree with Gerard's work completely.

## 6.0 CONCLUSION

A multi-node model has been developed for simulating the inflation process of conical parachute. Fluid-structure interaction in the inflation process of a selected parachute system was studied with dynamic equations derived from the multi-node model and CFD codes. The results are in good agreement with those from similar researches and relative experiments. The canopy breathing and the change of the vortex structure of the flow field in inflation process are discussed in detail.

## ACKNOWLEDGMENTS

A part of this work is financially supported by the National Natural Science Foundation of China (Grant 10577003) and Monash University of Australia, which is gratefully acknowledged.



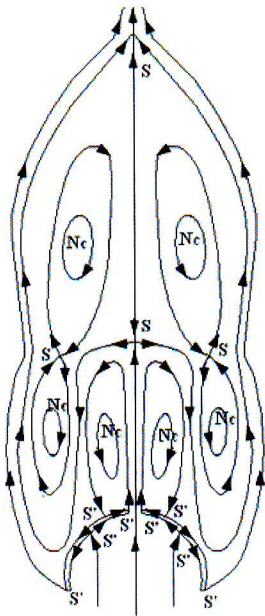


Figure 21. Topological structure of conical parachute flow field at quasi-steady stage.

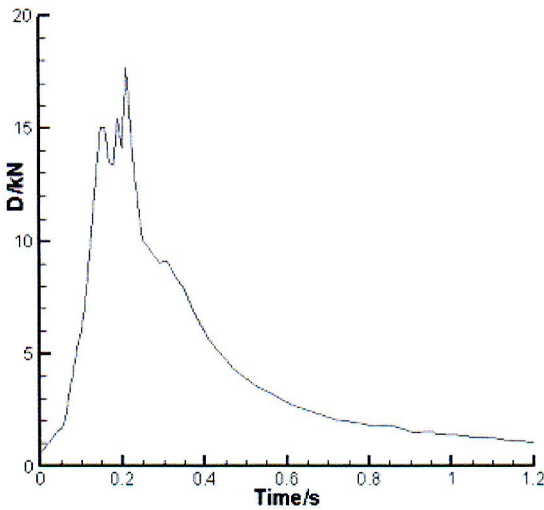


Figure 22. Change of inflation force.

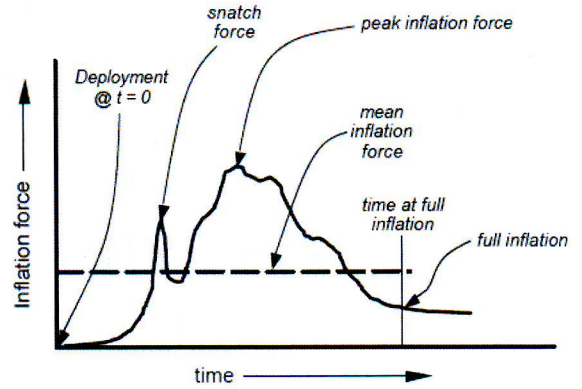


Figure 23. Time history of typical parachute inflation force<sup>(17)</sup>.

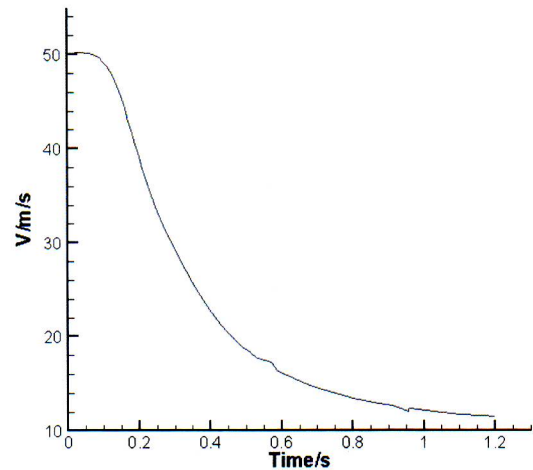


Figure 24. Change of descent velocity.

REFERENCES

1. STEIN, K.R., BENNEY, R.J., KALRO, V., JOHNSON, A.A. and TEZDUYAR, T.E. Parallel computation of parachute fluid-structure interactions, 1997, AIAA paper 1505.
2. STEIN, K.R., BENNEY, R.J., KALRO, V., TEZDUYAR, T.E., LEONARD, J. and ACCORSI, M. Parachute fluid-structure interactions: 3D computation, *Computer Methods in Applied Mechanics and Engineering*, 2000, **190**, pp 373-386.
3. PFLANZ, E. To determine the deceleration forces during the flowering of lifting parachutes, 1942, ZWB FB 1706.
4. O'HARA, F. Notes on the opening behavior and the open forces of parachutes, *Aeronaut J*, November 1949, **53**, (11), p 1053.
5. LUDTKE, W.P. A technique for the calculation of the opening-shock forces for several types of solid cloth parachutes, 1973, AIAA Paper 477.
6. LUDTKE, W.P. Notes on a generic parachute opening force analysis, 1986, NSWC TR No 142.
7. NORIO, A. and KENSAKU, S. Inflation process and free oscillation of flexible parachute-like body, 2005, AIAA paper 1610.

8. BENNEY, R.J. and STEIN, K.R. A computational fluid structure interaction model for parachute inflation, *J Aircr*, 1996, **33**, pp 730-736.
9. LINGARD, J.S. and DARLEY, M.G. Simulation of parachute fluid-structure interactions in supersonic flows, 2005, AIAA 1067.
10. STEIN, K., BENNEY, R., TEZDUYAR, T. and POTVIN, J. Fluid-structure interactions of a cross parachute: numerical simulation, *Computer Methods in Applied Mechanics and Engineering*, 2001, **191**, pp 673-687.
11. SURYANARANYANA, G.K. and PRABHU, A. Effect of natural ventilation on the boundary separation and near-wake vortex shedding characteristics of a sphere, *Experiments in Fluids*, 2000, **29**, p 582.
12. SURYANARANYANA, G.K. and MEIER G.E. A. Effect of ventilation on the flowfield around a sphere, *Experiments in Fluids*, 1995, **19**, pp 78-88.
13. EWING, E.G., BIXBY, H.W. and KNACKE, T.W. *Recovery System Design Guide*, 1978, Irvin Industries, California.
14. ZHU L. An approximate approach to calculate drag, stress and deformation of inflated flat circular parachute, *Landing Technology*, 1983, **1**, pp 143-177 (in Chinese) translated from Angenäherter Berechnung der Kräfte, Spannungen und Form des Ebenen Rundkappen-Fallschirms im gefüllten Zustand, DLR(FB) 71-98 Q(W) 0860.
15. JOHARI, H. and DESABRAIS, K.J. Vortex shedding in the near wake of a parachute canopy, *J Fluid Mech*, 2005, **536**, p 185.
16. TOBAK, M. and PEAKE D.J. Topology of three-dimensional separated flows, *Annual Review Fluid Mech*, 1982, **14**, pp 61-85.
17. WATKINS, J.W. A total energy method to predict parachute canopy inflation forces, 2003, AIAA paper 2166.
18. GARRARD, W.L. Application of inflation theories to preliminary parachute force and stress analysis, 1991, AIAA paper 0862-CP.